16th World Conference on Earthquake, 16WCEE 2017
Santiago Chile, January 9th to 13th 2017
Paper N° 1912
Registration Code: S-O1463281144

MAIN SHOCK-AFTERSHOCK SEQUENTIAL ANALYSIS ON REINFORCED CONCRETE COLUMNS

B. Kim(1) and M. Shin(2)

(1) Assistant Professor, Texas Tech University, byungmin.kim@ttu.edu
(2) Assistant Professor, Western New England University, moochul.shin@wne.edu

Abstract

This paper focuses on developing a main shock-aftershock (MSAS) sequential seismic analysis framework on reinforced concrete (RC) columns. Historical seismic events demonstrated the vulnerability of existing RC columns when they were subjected to a main shock followed by series of aftershocks. Especially, aftershocks during the 2011 Christchurch earthquake in New Zealand aggravated damages to Christchurch and the central city area economically and structurally. A series of aftershocks identified after a main shock caused severe damage on structures already weakened by the main shock. As there is growing attention to importance of aftershocks, a few main shock-aftershock sequential analyses have been suggested and developed. One of the common approaches to obtaining aftershock ground motion time series is to repeat main shock ground motion time series using frequency-invariant scaling factors. Another common approach is to randomly select time series from a set of main shock records and scaling them down to achieve desired amplitudes for aftershock motions. However, these conventional approaches are not capable of obtaining ground motion time series properly representing characteristics of aftershock ground motions because the frequency contents of aftershock ground motions usually differ from those of main shock ground motions. This research demonstrates the importance of properly representing aftershock ground motions in estimating the seismic responses of an RC column, and presents the differences in frequency contents between aftershock ground motions and the corresponding main shock ground motions. Time history seismic analyses are conducted using a finite element analysis program, OpenSees. The main shock motions recorded during the 1994 Northridge, California, and the 1997 Umbria Marche, Italy earthquakes are used. The aftershock motions are selected or obtained: (1) from recordings during the seismic events, (2) by scaling main shock motions to match the peak ground acceleration (PGA) values of aftershock motions, or (3) by spectrally matching main shock motions to the aftershock motions. The peak displacements and residual displacements of the column using the spectrally matched motions are closer to those results using real aftershock motion records, as compared to using the scaled motions. This demonstrates that the frequency contents of ground motions have significant impacts on the seismic responses of the RC column. Finally, in order to accommodate the forward prediction condition where aftershock ground motions are not available, an empirical relationship for the ratio of aftershock to main shock horizontal pseudo spectral accelerations (PSAs) at various periods is developed.

Keywords: RC column; main shock-aftershocks; nonlinear seismic analysis; NGA-West2;

1. Introduction

Recent earthquake events such as the 2011 Christchurch earthquake, New Zealand demonstrated the vulnerability of structures against sequential ground motions [1]. Therefore, it has been of great concern how to characterize and obtain realistic main shock-aftershock ground motions especially when conducting a seismic analysis of a structure. But, up to date, only a few methodologies have been developed and adopted for a seismic analysis under sequential ground motions: 1) One methodology for obtaining a sequential ground motion (MSAS) is to utilize actually recorded ground motions at a same station. Ruiz-García [2] conducted numerical analyses on structures using recorded main shock and aftershocks motions in Mexico, and reported that the structural behaviors would vary due to the different predominant periods in aftershock ground motions. Hatzigeorgiou and Liolios [3] obtained actual sequential seismic ground motion sets in the U.S. and performed seismic analyses of reinforced concrete (RC) frame structures against MSAS loadings. However, actual main shock and aftershock ground motion records are not always available for use especially for the forward prediction. 2) The other methodology, which has been adopted in a seismic sequential analysis, is to repeat main shock ground motions using frequency-invariant scaling factors [4]. 3) Another methodology relies upon randomly selecting ground motions among a set of traditional main shock records and scaling them up/down for their analyses in order to obtain sequential ground motions sets [5]. Those conventional means to acquire aftershock motions based on main shock motions with frequency-invariant scaling factors are limited to accurately estimate seismic performances of RC structures, because the frequency contents of aftershock records are usually different from those of main shock records.

Herein, the effects of frequency contents of aftershock ground motions on responses of a reinforced concrete (RC) column are explored. Main shock and aftershock earthquake ground motion pairs recorded during the 1994 Northridge earthquake, CA, the United States of America are chosen. A finite element program, OPENSEES is used to perform seismic analyses under multiple pairs of MSAS ground motions [6]. Structural responses using synthetic aftershock ground motions obtained by repeating/scaling main shock motions (a conventional method) and by spectrally matching main shock motions are compared to those using actual recorded MSAS ground motions. Furthermore, an empirical method to estimate aftershock ground motions is suggested for a situation where aftershock ground motions are not available for use.

2. Modeling and Validation

2.1 Modeling

A finite element program OpenSees was used to develop a numerical model of a reinforced concrete (RC) column, which is validated by a RC column test performed by Kawashima et al. [7,8]. A quasi-static cyclic testing was carried out. Fig. 1 shows schematics of the tested bridge column and its numerical model. The diameter of the tested circular column was 400 mm with 35 mm of the cover concrete. The effective height where the lateral cyclic force was applied at was 1,350 mm. 5% of the capacity of the RC cross-section was applied as an axial loading. The compressive strength of concrete, and the yield strengths of the longitudinal and lateral reinforcement were 30 MPa, 374 MPa and 363 MPa, respectively. More details of the tested column can be found in their study [7]. For the numerical model, total four nonlinear displacement-based beam-column elements were used (EL1~EL4). Nonlinear constitutive material models were assigned to core concrete (modified-Concrete01), cover concrete (modified-Concrete01) and longitudinal reinforcement (Steel 02), respectively using a fiber section analysis. The main failure mechanism of the numerical column is the rupture of confinements, which is implemented in modified-Concrete01. Fig.1.(d) shows the failure mode observed during the test [8]. An elastic beam-column element was selected for the top portion of the column, EL5. A lumped mass of 18,858 kg was assigned to the top node of the column, which represent a super structure. More details of the numerical model can be found in the previous study [9]. The numerical model was subjected to the same

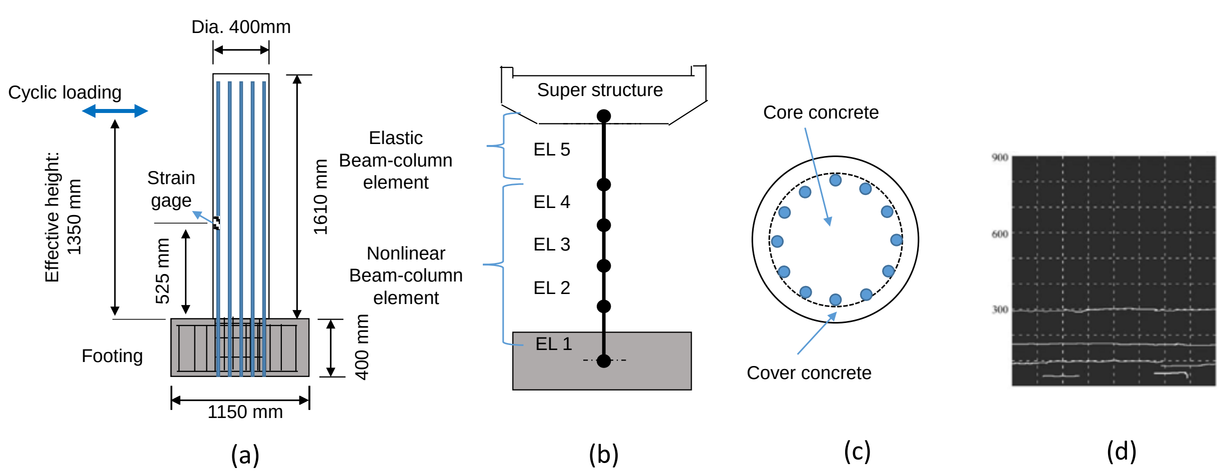

Fig. 1– Schematics of the tested column (a), numerical model (b), the cross section of the column (c), and damage of the tested column (d) [8].

cyclic loading protocol that was adopted during the experimental test. 0.5%-drift of the increment cyclic loading was applied until the drift reached 5 %. Fig. 2 compares the force-displacement relationships between the experiment and numerical analysis. The results of the numerical analysis agreed with the experimental results in terms of its strength, loading and unloading paths. The maximum lateral force of the numerical result was 4% higher than that of the experimental column. Especially local strain values were also compared with the strain values obtained from one strain gage placed on the longitudinal reinforcement at the height of 525 mm from the top of the footing.

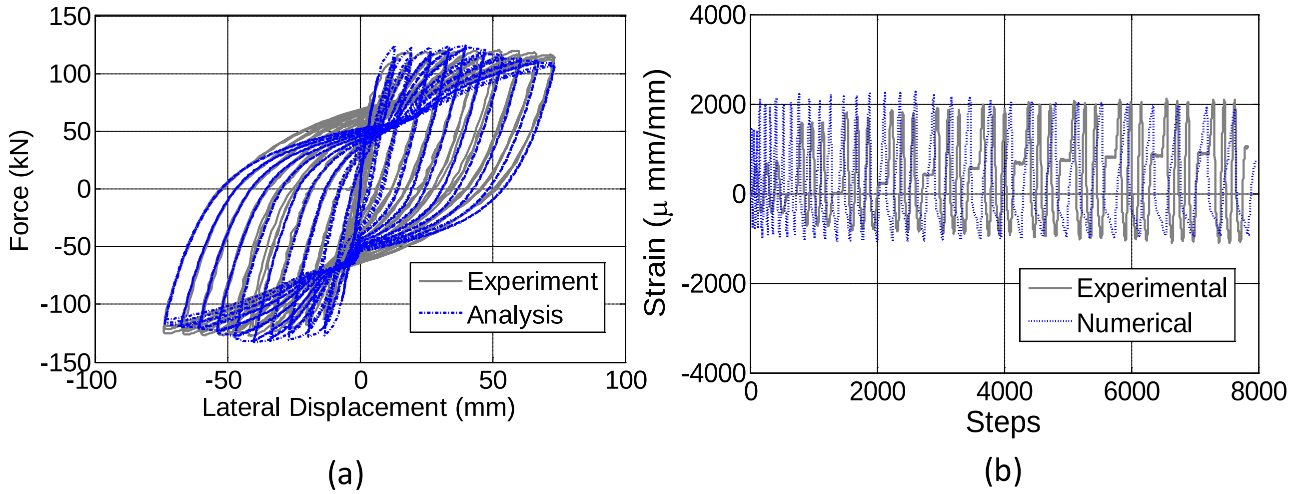

Fig. 2 - Comparison of the force-displacement relationships (a) and the strain values of one of the longitudinal reinforcement (b)

3 Selected Main shock-Aftershock Ground Motions

A number of ground motions recorded during the **M**6.7 1994 Northridge, California, the United States of America and the **M**6.0 1997 Umbria-Mache, Italy, earthquakes were collected from the Next Generation Attenuation relationships for Western U.S. (NGA-West2) database [10]. Aftershock ground motions recorded at the stations at which the selected main shock motions were recorded were also selected. Total 10 main shock-aftershock ground motion sets were selected for the analyses. Table 1 summarizes the magnitudes and record sequence number (RSN) of the selected main shock-aftershock pairs. Fig. 3 shows ratios of spectral accelerations (*Sa*) of the selected aftershocks to those of the corresponding main shocks. The spectral accelerations were normalized by peak ground accelerations (PGA) to evaluate the variation of spectral accelerations at different periods. It is worth noting that *Sa* of aftershocks (Sa^{AS}) is generally smaller than those of main shocks (Sa^{MS}) at periods longer than approximately 2.0 sec. The predominant period is a period at which the maximum spectral acceleration occurs in an acceleration response spectrum calculated at 5% damping. The mean period can be estimated by the following equation:

$$T_m = \frac{\sum C_i^2 / f_i}{\sum C_i^2} \quad , \tag{1}$$

where C_i is the Fourier amplitude, and f_i represents the discrete Fourier transform frequencies between 0.25 and 20 Hz.

4. Main shock-Aftershock Sequential Analysis

A series of nonlinear time history analyses were conducted on the validated numerical RC column model. The numerical model was subjected to three different sequential ground motions: (1) actual main shock and after shock ground motions recorded at same stations (MS-AS), (2) repeating/scaling main shocks to represent aftershocks (MS-MS), or (3) spectrally matching main shock motions to the aftershock motions (MS-SM). The maximum displacement and the relative residual displacement (i.e. the 2nd residual displacement – 1st residual displacement) during these three sequential ground motions were considered as seismic responses.

The main shock ground motions were spectrally matched to the aftershock ground motions by using a program, SeismoMatch [11] over a period range of 0.02 sec through 2.00 sec. Fig. 4 shows main shock and aftershock motions of the **M**6.7 Northridge, California, earthquake recorded at the LA-Sepulveda VA Hospital station, as well as those of the main shock motion spectrally matched to the aftershock motion. The spectral shape of the aftershock motion is quite different from that of the main shock motion. The spectrally matched main shock motion is similar to the aftershock motion over an entire period range.

Table 1- Selected sequential main shock-aftershock pairs with record sequence numbers (RSN) of the NGA-West2 database.

Earthquake Name	Main shock Magnitude	Main shock RSN	Aftershock Magnitude	Aftershock RSN	Station Name
1994 Northridge	6.7	1004	5.3	3771	LA - Sepulveda VA Hospital
1994 Northridge	6.7	1039	6.0	1681	Moorpark - Fire Sta
1994 Northridge	6.7	1044	5.2	1670	Newhall - Fire Sta
1994 Northridge	6.7	1052	5.2	1671	Pacoima Kagel Canyon
1994 Northridge	6.7	1085	5.3	1737	Sylmar - Converter Sta East
1994 Northridge	6.7	1086	5.3	3767	Sylmar - Olive View Med FF
1997 Umbria Marche, Italy	6.0	4349	5.5	4364	Colfiorito
1997 Umbria Marche, Italy	6.0	4349	5.6	4385	Colfiorito
1997 Umbria Marche, Italy	6.0	4345	5.5	4362	Assisi-Stallone
1997 Umbria Marche, Italy	6.0	4352	5.5	4367	Nocera Umbra

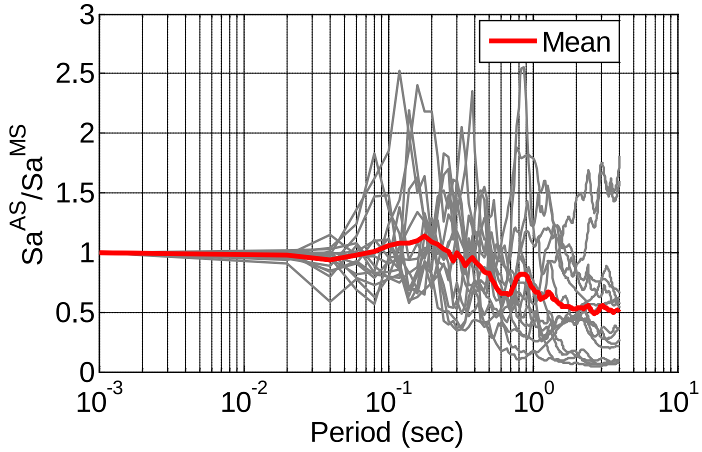

Fig. 3 - Ratios of spectral accelerations of aftershocks (Sa^{AS}) to those of main shocks (Sa^{MS}) after normalizing them by PGA values. The red line represents a mean ratio.

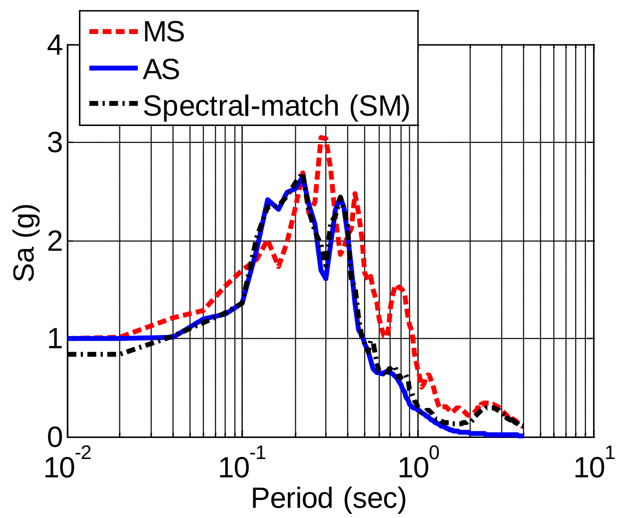

Fig. 4 - Main shock and aftershock spectral accelerations of the **M**6.7 Northridge, California, earthquake recorded at the LA-Sepulveda VA Hospital station, as well as that of the main shock motion spectral matched to the aftershock motion.

4.1 Scaled to 1 g of PGA

The main period (T1) of Kawashima et al's column was found to be 0.18 seconds when 10% of the compressive strength of the cross section was assigned to the top node representing the weight of the super structure. All of the selected main shock and aftershock ground motions were scaled to have the peak ground acceleration (PGA) of 1 g. Fig. 5 shows seismic responses of the RC column model subjected to three sets of main shock-aftershock ground motions: MS-AS; MS-MS; and MS-SM for the 1944 Northridge earthquake. The RSNs for main shock and aftershock ground motions are 1004 and 3771, respectively. The main shock ground motions are identical for the three sets of the sequential ground motions, and followed by three different aftershock ground motions. Fig. 5 clearly shows the differences between the seismic responses of the RC column when it was subjected to the actual sequential ground motions (MS-AS) and the main shock ground motion followed by the synthetic aftershock ground motion generated by repeating the main shock motion (MS-MS). After the main shock ground motion, the first residual displacement is found to be 10.82 mm for all three cases (Fig. 5.a). Then, the 2nd residual displacements of the RC column after three different aftershock motions are 8.80 mm (MS-AS), 13.69 mm (MS-MS) and 10.57 mm (MS-SM), respectively. The 2nd residual displacement under MS-AS is shifted toward the original position by 2.02 mm. However, the 2nd residual displacement under MS-MS is shifted to the other direction by 2.87 mm. Furthermore, the maximum displacements under MS-AS and MS-MS are quite different; 56.80 mm (MS-AS) and 80.82 mm (MS-MS) respectively. The seismic responses of the column are overestimated when it was subjected to a sequential ground motion set using a traditional method as compared to that under the actual main shock-aftershock ground motion. This was due to the fact that the RC column's main period changed when subject to a main shock ground motion and the frequency contents of aftershock ground motions affected the response of the RC column. When the main shock motion is spectrally matched to the aftershock motion, the frequency contents of spectrally matched motion become similar to those of the aftershock motion. The maximum and final residual displacements recorded under MS-SM are found to be 52.41 and 10.57 mm, respectively, which are closer to those using MS-AS rather than using MS-MS. Similar observations are found in the lateral force and displacement relationships (Fig. 5.b). This clearly demonstrates the importance of properly characterizing the frequency contents of aftershock ground motions for main shock-aftershock sequential analyses.

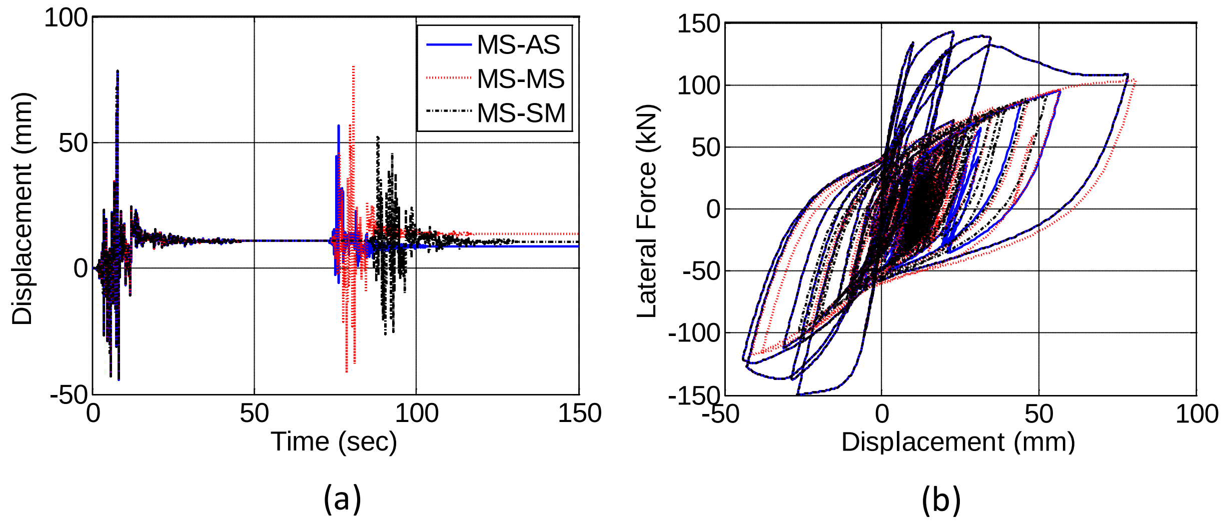

Fig. 5 - Seismic responses of the RC column model under the **M**6.7 1994 Northridge main shock and aftershock ground motions recorded at the LA – Sepulveda VA Hospital station: (a) time histories of the top displacement, and (b) the lateral force and displacement relationships.

4.2 Scaled to the spectral acceleration of 1 g

The ground motions were scaled to match the spectral acceleration of 1 g at the main period of the original column (T1 = 0.18 sec) in order to further examine the effects of the frequency contents on the seismic responses of the RC column. Fig. 6 shows the time history displacements of the RC column under three sets of earthquake sequential ground motions from the 1994 Northridge, USA and 1997 Umbria-Marche, Italy earthquakes. The results using the spectrally matched ground motions (MS-SM) are closer to those using the actual main shock-after shock sequential records (MS-AS). This phenomenon becomes more pronounced when the RC column got more damaged by the main shocks. When the damage is minor, the differences between MS-AS, MS-MS and MS-SM are minimal, since the structure still behaves elastically, and the change of the main period of the structure is insignificant.

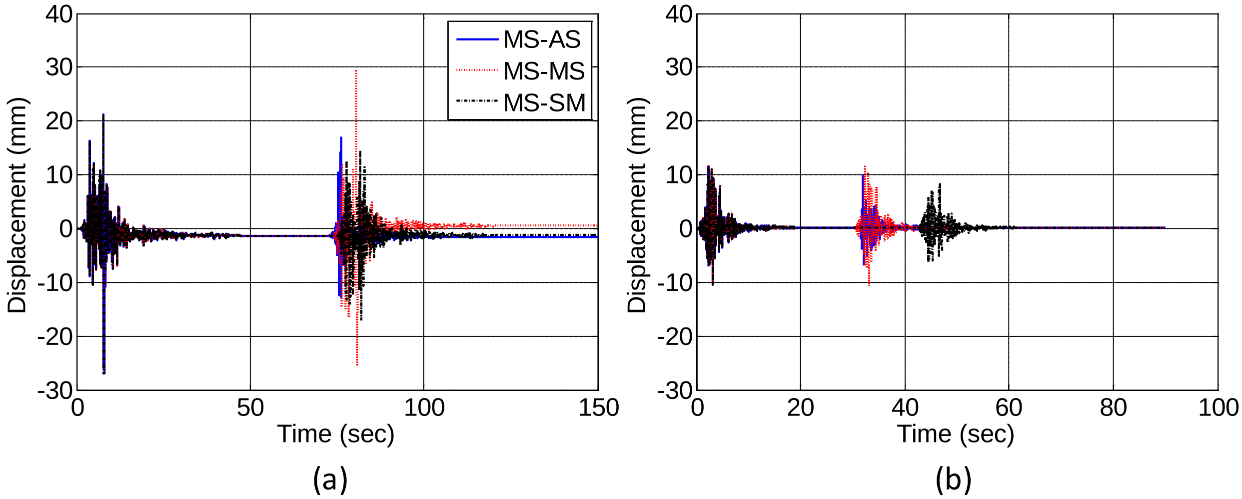

Fig. 6 - Time history displacements of the RC column under: (a) the 1994 Northridge motions at the LA – Sepulveda VA Hospital station and (b) the 1997 Umbria-Marche motions at the Nocera Umbra station.

4.3 Summary of the numerical simulations

Fig. 7 shows that the maximum displacements during the aftershocks using the MS-MS method are much higher than those using the MS-AS and MS-SM methods, especially when the ratio of mean periods ($T_{m\text{-}AS}/T_{m\text{-}MS}$) is less than 0.9 (see Fig. 7.a). The average ratio of the maximum displacements due to MS-MS to MS-AS ($\text{MaxDispl.}_{\text{MS-MS}}/\text{MaxDispl.}_{\text{MS-AS}}$) is found to be 134.48% while that of the maximum displacement due to MS-SM to MS-AS was 97.84%. The ratios of maximum displacements using the MS-MS method to those using the MS-AS method tend to increase as $T_{m\text{-}AS}/T_{m\text{-}MS}$ decreases, which clearly indicates the effects of frequency contents in main shock and aftershock ground motions on structural responses. However, when the spectrally matched main shock ground motions are used for the aftershock ground motions (the MS-SM method), the maximum displacement ratio does not vary much with respect to $T_{m\text{-}AS}/T_{m\text{-}MS}$. This is because the frequency contents of the main shock ground motions are matched with those of actual aftershock ground motions during the spectral matching procedure. The relative residual displacements during the aftershock ground motions were also investigated and summarized in Fig. 7.b. A ratio of 100 % means that the relative residual displacement due to either MS-MS or MS-SM is identical to the relative residual displacements observed under the actual aftershocks records (MS-AS). The figure indicates the results using the spectral-match method are closer to the 100 % line as compared with the results using MS-MS. More than 50% of the results based on MS-MS exhibits negative ratios, which indicates that the residual displacements using MS-MS for the aftershocks are shifted to the opposite direction of the 2nd residual displacements overserved using MS-AS.

In order to accurately estimate seismic responses of structures under sequential ground motions, a frequency-dependent scaling factor is recommended, especially when shorter mean periods are expected for aftershock ground motions compared to those for main shock motions.

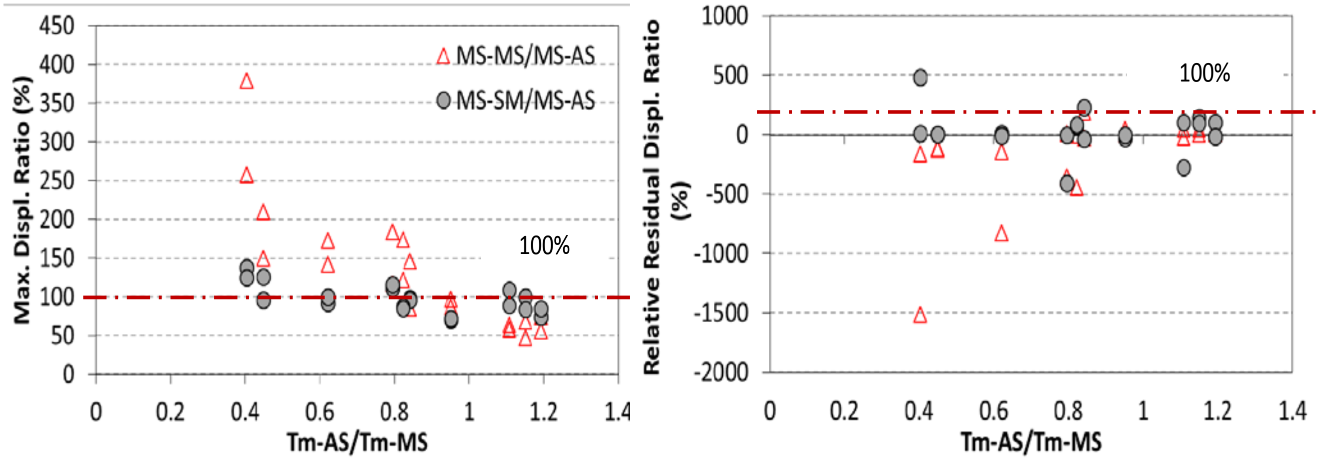

Fig. 7 - The ratio of the absolute maximum displacements (a) and the relative residual displacement ratio during the aftershocks (b) with respect to $T_{m\text{-}AS}/T_{m\text{-}MS}$

5. Frequency-Dependent Aftershock Ground Motion Estimation Model

5.1 Ratio of PSAs of aftershocks to main shocks

Ground motion data in active crustal regions (ACRs) were selected from the Next Generation Attenuation relationships for the Western United States (NGA-West2) database [10]. Aftershock events were defined as those having a Centroid Joyner-Boore distance (CR_{JB}) less than 20 km [12]. The data set used in this study consists of 2,817 pairs of main shock and aftershock ground motions (recorded at the same stations) from 140 aftershocks and 39 main shocks. Among these records, 490 pairs are from the state of California, U.S.A, 100 pairs from the Mediterranean region (Italy and Turkey), 923 pairs from China, 1,303 pairs from Taiwan, and one from Nicaragua.

Magnitudes of the main shock earthquakes range from 3.2 to 7.9, while those of the aftershock earthquakes range from 3.0 to 7.1. The range of the rupture distances of the main shock records is from 1.6 to 473 km, while those of the aftershock records from 3.8 to 496 km. Values of time-averaged shear-wave velocities for the top 30 m soil deposits (V_{S30}) at the selected recording stations vary from 124 m/s to 1,526 m/s. The 5% damped pseudo spectral accelerations (PSAs) at 15 oscillator periods (T) from 0.01 s to 10 s were used. These ground motion intensity measures are obtained by averaging two horizontal ground motion records.

This study systematically investigates the relationships between PSA^{AS}/PSA^{MS} and three important factors: 1) the ratio of aftershock magnitude to main shock magnitude ($\mathbf{M}^{AS}/\mathbf{M}^{MS}$), 2) the ratio of rupture distances ($R_{rup}^{AS}\big/R_{rup}^{MS}$), and 3) the V_{S30} at a recording station. Fig. 8 shows PSA^{AS}/PSA^{MS} with respect to magnitude ratio ($\mathbf{M}^{AS}/\mathbf{M}^{MS}$) for the four selected periods. The mean values and mean ± one standard deviation of $\ln(PSA^{AS}/PSA^{MS})$ grouped by uniformly spaced $\mathbf{M}^{AS}/\mathbf{M}^{MS}$ bins are plotted. The $\ln(PSA^{AS}/PSA^{MS})$ decreases as the magnitude ratio decreases. The decreasing rate is faster at longer periods. When magnitudes of aftershocks and main shocks are similar to each other, the PSA^{AS}/PSA^{MS} ratios are close to 1 (since $\ln(PSA^{AS}/PSA^{MS}) = 0$). However, when the magnitude of aftershock is 75% of the magnitude of main shock, the PSA^{AS}/PSA^{MS} ratio changes with a greater rate. When the magnitude of aftershock is about 50 % of the magnitude of main shock, the pseudo spectral acceleration of aftershock is found to be less than 2 % of that of main shock at short periods and less than 1 % at long periods.

5.2 Predictive model

This study proposes a predictive model for estimating ground motion intensity measures for aftershock earthquakes given the information of main shock earthquakes and sites of interest. Therefore, the three most important variables (i.e., magnitude ratio, distance ratio, and V_{S30}) are considered.

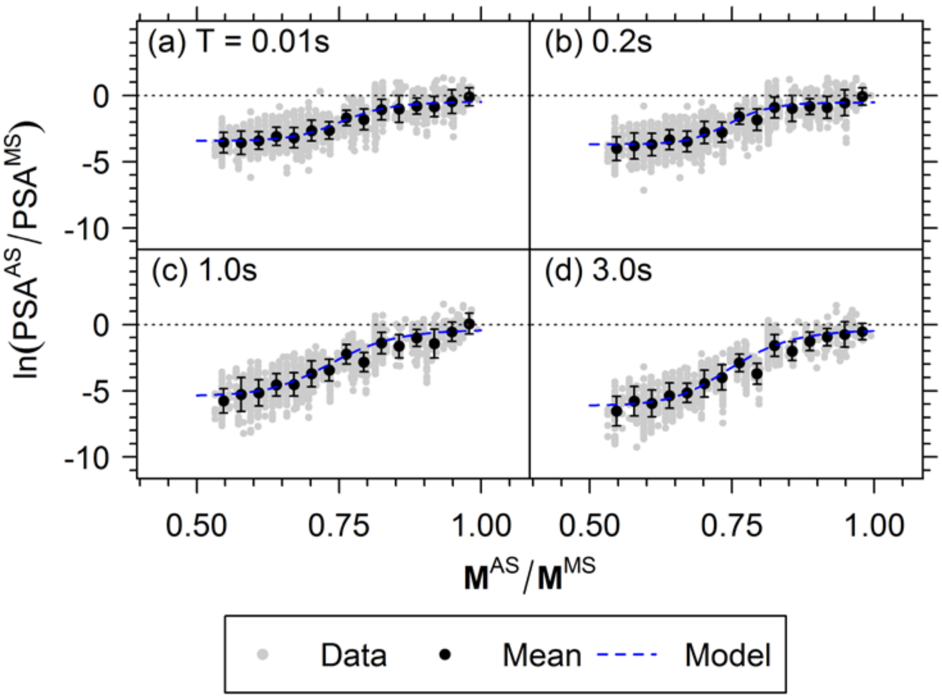

Fig. 8 - Natural logarithm of PSA^{AS}/PSA^{MS} with respect to magnitude ratio ($\mathbf{M}^{AS}/\mathbf{M}^{MS}$) for four selected periods. Mean and mean ± one standard deviation (as error bars) grouped by magnitude ratio bins are shown. The model for a condition of $R_{rup}^{AS}/R_{rup}^{MS}$ =1.5 and V_{S30} = 350 m/s is compared.

5.2.1 Functional form of the model

The model for the aftershock scaling factor is given by:

$$\ln\left(\frac{PSA^{AS}}{PSA^{MS}}\right) = c_0 + c_1 \frac{\left(M^{AS}/M^{MS}\right)^{C_3}}{c_2 + \left(M^{AS}/M^{MS}\right)^{C_3}} + c_4 \ln\left(\frac{R_{rup}^{AS}}{R_{rup}^{MS}}\right) + c_5 \ln\left(V_{S30}\right) \tag{2}$$

where the superscripts, AS and MS, denote aftershock and main shock, respectively. c_0 through c_5 are the regression coefficients. The magnitude ratio scaling term is used to capture the varying slopes of $\ln(PSA^{AS}/PSA^{MS})$ versus $\mathbf{M}^{AS}/\mathbf{M}^{MS}$. Log-linear relationships for the distance ratio ($R_{rup}^{AS}/R_{rup}^{MS}$) and V_{S30} are used to capture the trends for the majority of the data, while maintaining the simplicity of the model.

Regression analyses were performed at each period, and the obtained coefficients were smoothed especially at long periods to minimize the jaggedness caused by the lack of data due to frequency filtering, and to achieve smooth aftershock scaling factors with respect to period. The final set of smoothed coefficients is provided in Table 2. The model for $\ln(PSA^{AS}/PSA^{MS})$ is plotted in Fig. 8 with respect to magnitude ratio for representative values of a distance ratio and V_{S30} ($R_{rup}^{AS}/R_{rup}^{MS}$ =1.5 and V_{S30} = 350 m/s) for the four selected periods. The model catches a trend of variable slopes in the data.

Fig. 9 shows PSA^{AS}/PSA^{MS} versus period estimated by the proposed model for various magnitude ratios, distance ratios, and V_{S30} values. It clearly shows strong dependency of PSA^{AS}/PSA^{MS} on the period and magnitude ratio. The PSA^{AS}/PSA^{MS} increases with the magnitude ratio, and it decreases with the period (T) at T > ~ 0.25 s when $\mathbf{M}^{AS}/\mathbf{M}^{MS}$ = 0.85, and at T > ~ 0.1 s when $\mathbf{M}^{AS}/\mathbf{M}^{MS}$ = 0.70. The PSA^{AS}/PSA^{MS} decreases with the distance ratio and V_{S30}.

Table 2. Regression coefficients (c_0 through c_5)

Period (sec)	c_0	c_1	c_2	c_3	c_4	c_5
0.01	-1.24297	2.9497	0.00854	17.0188	-0.3541	-0.3435
0.02	-1.22781	2.9453	0.00859	16.9919	-0.3647	-0.3447
0.03	-1.16205	2.8997	0.00794	17.3751	-0.3835	-0.3480
0.05	-0.93098	2.7522	0.00675	18.1163	-0.3811	-0.3648
0.1	-1.00299	2.6994	0.00263	21.1454	-0.2851	-0.3607
0.2	-1.36775	3.1518	0.00264	20.2310	-0.3714	-0.3722
0.3	-1.54502	3.4626	0.00386	18.5709	-0.3755	-0.4051
0.4	-1.83319	3.8233	0.00617	17.0427	-0.3754	-0.4195
0.5	-2.08245	4.0729	0.00946	15.7773	-0.3767	-0.4207
1	-2.88502	5.0222	0.01915	13.0716	-0.3807	-0.4218
2	-3.4969	5.7010	0.01981	13.2437	-0.4799	-0.4187
3	-3.64788	5.7171	0.01750	14.0292	-0.5908	-0.4119
4	-3.68629	5.3452	0.00830	16.5712	-0.6651	-0.3902
5	-3.8765	5.1454	0.00458	18.8002	-0.6994	-0.3693
10	-4.29002	4.5459	0.00097	24.4269	-0.7105	-0.2854

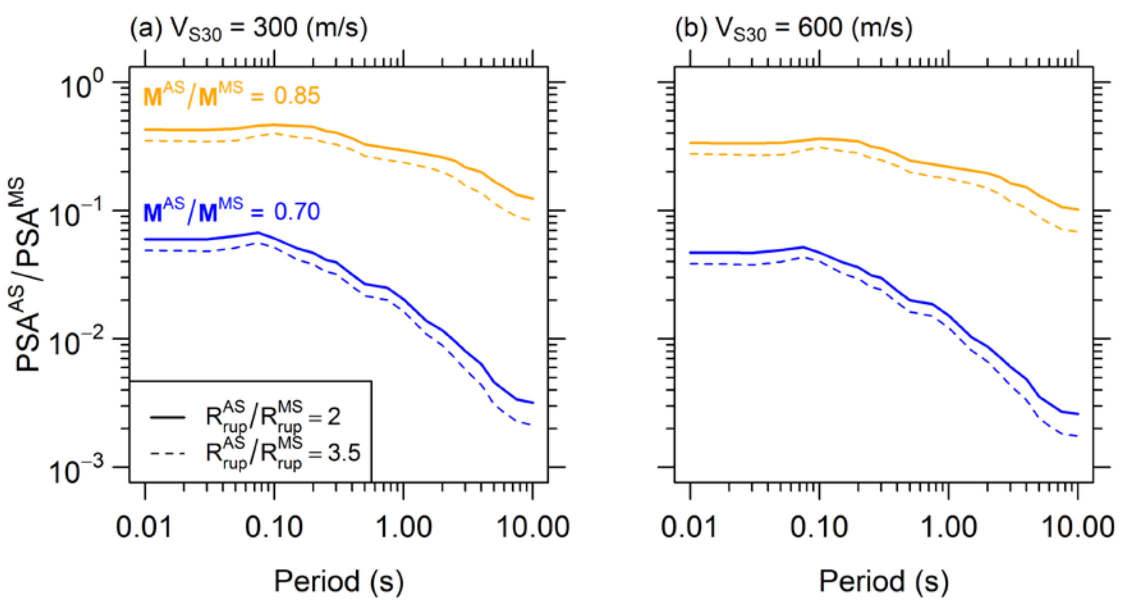

Fig. 9 - The PSA^{AS}/PSA^{MS} model as a function of period estimated by the proposed model with various magnitude ratios and distance ratios, and for two site conditions: (a) V_{S30} = 300 m/s; and (b) V_{S30} = 600 m/s.

6. Conclusions

Generating realistic sequential earthquake ground motions is of great concern in the earthquake engineering practice, in order to ensure the integrity of infrastructure and accurately estimate structural responses. Up to date, researchers have synthesized aftershock motions based on main shock ground motions using frequency-invariant scaling factors or randomly choosing different main shock motions. However, recent studies have demonstrated that aftershock ground motions should be differentiated from main shock ground motions due to their different mechanisms. The first part of this research focused on investigating the effects of the frequency contents on responses of a RC numerical column model. Three different methods were used to generate/obtain aftershock ground motions: 1) actual aftershock ground motion records (MS-AS); 2) repeating/scaling main shock ground motions with frequency-invariant scaling factors (MS-MS); and 3) spectrally matching main shock ground motions to corresponding aftershock ground motions (MS-SM). Nonlinear time history analyses were conducted on the numerical model using these actual and synthesized sequential ground motions sets. The results clearly demonstrated that the frequency contents of the ground motions played significant role on the responses of the RC column. When using the traditional method (MS-MS), the maximum displacements tend to be overestimated as compared to those due to the actual recorded sequential ground motions (MS-AS). In addition, the residual displacements using MS-MS were estimated to be in the opposite direction to those using MS-AS when the columns' main period (T1) is shorter than mean periods of main shock motions (T_m). These differences became pronounced when the mean period of the aftershock ground motions are less than those of the main shock ground motions. When main shock ground motions spectrally matched to aftershock motions were used (MS-SM), the responses of the RC column were much closer to those using actual ground motion records (MS-AS). Therefore, the period-dependent scaling is recommended to generate aftershock motions for main shock-aftershock sequential analyses, especially when shorter predominant and mean periods are expected for aftershock ground motions compared to those for main shock motions.

The second part of the study presented an empirical model to estimate aftershock scaling factors, PSA^{AS}/PSA^{MS} at various periods. This study aimed to demonstrate the characteristics of aftershock ground motions that are different from main shock ground motions. 2,817 main shock-aftershock paired records at the same stations were selected from the NGA-West2 database. A predictive model of aftershock scaling factors (PSA^{AS}/PSA^{MS}) was developed using three important variables: earthquake magnitude ratio ($\mathbf{M}^{AS}/\mathbf{M}^{MS}$), rupture distance ratio ($R_{rup}^{AS}/R_{rup}^{MS}$), and V_{S30}. Among these variables, the aftershock scaling factor is most strongly dependent on the magnitude ratio. The aftershock scaling factor decreases with decreasing magnitude ratio, and the decreasing rate becomes faster at long periods. The scaling factor decreases with the distance ratio and V_{S30}.

7. References

[1] Elnashai AS, Gencturk B, Kwon O-S, Al-Qadi IL, Hashash Y, Roseslor JR, Kim SJ, Jeon S-H, Dukes J, Valdivia A (2010): The Maule (Chile) Earthquake of February 27, 2010 - Consequence Assessment and Case Studies, in, *Mid-America Earthquake Center*, 190.

[2] Ruiz-García J (2012): Mainshock-Aftershock Ground Motion Features and Their Influence in Building's Seismic Response. *Journal of Earthquake Engineering*, **16**, 719-737.

[3] Hatzigeorgiou GD, Liolios AA (2010): Nonlinear behaviour of RC frames under repeated strong ground motions. *Soil Dynamics and Earthquake Engineering*, **30**, 1010-1025.

[4] Li Q, Ellingwood BR (2007): Performance evaluation and damage assessment of steel frame buildings under main shock–aftershock earthquake sequences. *Earthquake Engineering & Structural Dynamics*, **36**: 405-427.

[5] Luco N, Bazzurro P, Cornell A (2004): Dynamic versus static computation of the residual capacity of a mainshock-damged building to withstand an aftershock. *13th World Conference on Earthquake Engineering*, Vancouver, B.C., Canada.

[6] Mazzoni S, McKenna F, Scott MH, Fenves GL et al. (2009): OpenSees Command Language Manual. *Open System for Earthqauke Engineering Simluations*.

[7] Kawashima K, Hosotani M, Yondea K (2001): Carbon fiber sheet retrofit of reinforced concrete bridge piers toward new generation seismic design methodology of bridges. *Tokyo Institute of Technology*, Tokyo, Japan

[8] Yoneda K, Kawashima K, Shoji G. (2001): Seismic Retrofit of Circular Reinforced Bridge Columns by Wrapping of Carbon Fiber Sheets. Proceeding of JSCE, **682**, 41-56.

[9] Andrawes B, Shin M, Wierschem N. (2010): Active Confinement of Reinforced Concrete Bridge Columns Using Shape Memory Alloys. *Journal of Bridge Eng ASCE*, **15**, 81-89.

[10] Ancheta TD, Darragh RB, Stewart JP, Seyhan E, Silva WJ, Chiou BS-J, Wooddell KE, Graves RW, Kottke AR, Boore DM, Kishida T, Donahue JL (2014): NGA-West2 Database, *Earthquake Spectra*, **30**, 989-1005.

[11] Seimosft (2015). SeismoMatch, V2.1.2, http://www.seismosoft.com/

[12] Wooddell, KE and NA Abrahamson, Classification of Main Shocks and Aftershocks in the NGA-West2 Database. Earthquake Spectra, (2014). 30(3): p. 1257-1267.